The inverse scattering problem for a homogeneous bi-isotropic slab using transient data

Kristensson, Gerhard; Rikte, Sten

1992

CODEN:LUTEDX/(TEAT-7022)/1-13/(1992)

The inverse scattering problem for a homogeneous bi-isotropic slab using transient data

Gerhard Kristensson and Sten Rikte

Department of Electroscience
Electromagnetic Theory
Lund Institute of Technology
Sweden

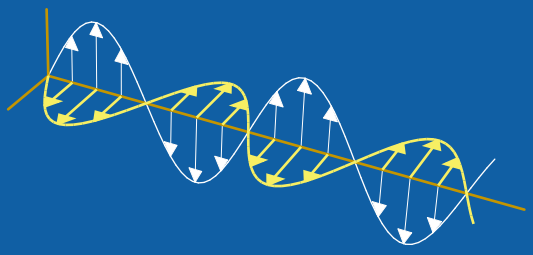

Gerhard Kristensson
Sten Rikte

Department of Electromagnetic Theory
Lund Institute of Technology
P.O. Box 118
SE-221 00 Lund
Sweden

Editor: Gerhard Kristensson

Abstract

Transient wave propagation in a finite bi-isotropic slab is treated. The incident field impinges normally on the slab, which can be inhomogeneous wrt depth. Dispersion and bi-isotropy are modeled by time convolutions in the constitutive relations. Outside the slab the medium is assumed to be homogeneous, non-dispersive and isotropic, and such that there is no phase velocity mismatch at the boundaries of the slab. Two alternative methods of solution to the propagation problem are given—the imbedding method and the Green function approach. The second method is used to solve the inverse problem and the first to generate synthetic data. The inverse scattering problem is to reconstruct the four susceptibility kernels of the medium using a set of finite time trace of reflection and transmission data.

1 Basic equations

The wave propagation problem in bi-isotropic media has received extensive attention during recent years. The fixed frequency problem has been analyzed by many authors, see [3, 10] for a review of recent work. Transient problems have also been addressed, see [8, 9]. The present analysis of the transient problem is a generalization of previous work for the isotropic slab, see Ref. [7], and applies the generalization of the wave splitting technique to the Maxwell equations [12].

Consider a dispersive bi-isotropic slab with boundaries, $z = 0$ and $z = d$. The slab can be inhomogeneous in the z-direction. Outside the slab, the medium is assumed to be non-dispersive with constant permittivity $\epsilon_0\epsilon$ and permeability $\mu_0\mu$. The phase velocity c and the wave impedance η of the surrounding medium is then given by

$$c = \frac{1}{\sqrt{\epsilon_0\epsilon\mu_0\mu}} = \frac{c_0}{\sqrt{\epsilon\mu}}, \qquad \eta = \sqrt{\frac{\mu_0\mu}{\epsilon_0\epsilon}} = \eta_0\sqrt{\frac{\mu}{\epsilon}}$$

respectively[1]. The slab is assumed to have no mismatch at the boundaries, $z = 0$ and $z = d$. The appropriate constitutive relations used in this paper are, see Ref. [6, 9][2]:

$$\begin{cases} c\eta \boldsymbol{D}(\boldsymbol{r},t) = \boldsymbol{E}(\boldsymbol{r},t) + ((G+F)*\boldsymbol{E})(\boldsymbol{r},t) + \eta((K+L)*\boldsymbol{H})(\boldsymbol{r},t) \\ c\boldsymbol{B}(\boldsymbol{r},t) = ((-K+L)*\boldsymbol{E})(\boldsymbol{r},t) + \eta\boldsymbol{H}(\boldsymbol{r},t) + \eta((G-F)*\boldsymbol{H})(\boldsymbol{r},t) \end{cases} \tag{1.1}$$

where time convolution is denoted by $*$, i.e.

$$(G*\boldsymbol{E})(\boldsymbol{r},t) = \int_{-\infty}^{t} G(z,t-t')\boldsymbol{E}(\boldsymbol{r},t')\,dt'$$

The kernels G and F model the ordinary dispersive effects, while K and L model the bi-isotropy of the medium. If $L = 0$, the medium is reciprocal [6]. Causality implies that the functions G, F, K and L are identically zero for $t < 0$. Furthermore, all

[1]The subscript zero indicates the corresponding vacuum values.

[2]Note the change in notation between this paper and these references.

kernels are assumed to be continuously differentiable functions of t for $t > 0$ at each point $\boldsymbol{r}$ in the interior of the slab. Outside the slab, G, F, K and L are all identical to zero.

The slab is excited by a (known) general plane wave, with electric field $\boldsymbol{E}_i$, propagating in the positive z-direction. Moreover, the electric field $\boldsymbol{E}$ is everywhere assumed to be of the form

$$\boldsymbol{E}(\boldsymbol{r}, t) = \boldsymbol{e}_x E_x(z, t) + \boldsymbol{e}_y E_y(z, t)$$

and similarly for the other electromagnetic vector fields[3]. Thus, by introducing the reflected, $\boldsymbol{E}_r$, and the transmitted, $\boldsymbol{E}_t$, electric fields, respectively, the total electric field outside the slab can be written as

$$\boldsymbol{E}(z, t) = \begin{cases} \boldsymbol{E}_i(z, t) + \boldsymbol{E}_r(z, t), & z \leq 0 \\ \boldsymbol{E}_t(z, t), & z \geq d \end{cases}$$

The source free Maxwell equations are the basic equations that model the dynamics of the electromagnetic fields.

$$\nabla \times \boldsymbol{E}(\boldsymbol{r}, t) = -\frac{\partial \boldsymbol{B}(\boldsymbol{r}, t)}{\partial t}$$
$$\nabla \times \boldsymbol{H}(\boldsymbol{r}, t) = \frac{\partial \boldsymbol{D}(\boldsymbol{r}, t)}{\partial t}$$

It is convenient to use a matrix notation and, therefore, vectors in the x-y-plane are identified with their column vector representations, i.e.

$$\boldsymbol{E}(\boldsymbol{r}, t) = \begin{pmatrix} E_x(z, t) \\ E_y(z, t) \end{pmatrix}$$

The Maxwell equations can then be written

$$\frac{\partial}{\partial z} \begin{pmatrix} \boldsymbol{E} \\ \eta \mathbf{J} \boldsymbol{H} \end{pmatrix} = \frac{1}{c} \frac{\partial}{\partial t} \begin{pmatrix} c\mathbf{J}\boldsymbol{B} \\ c\eta \boldsymbol{D} \end{pmatrix}$$

where $\mathbf{J}$ is defined by

$$\mathbf{J} = \begin{pmatrix} 0 & -1 \\ 1 & 0 \end{pmatrix}$$

The constitutive relations (1.1) are now used to eliminate the $\boldsymbol{D}$ and the $\boldsymbol{B}$-fields in this equation. The result is

$$c\frac{\partial}{\partial z} \begin{pmatrix} \boldsymbol{E} \\ \eta \mathbf{J} \boldsymbol{H} \end{pmatrix} = \begin{pmatrix} (-\mathbf{K} + \mathbf{L})* & \mathbf{I} + (\mathbf{G} - \mathbf{F})* \\ \mathbf{I} + (\mathbf{G} + \mathbf{F})* & -(\mathbf{K} + \mathbf{L})* \end{pmatrix} \frac{\partial}{\partial t} \begin{pmatrix} \boldsymbol{E} \\ \eta \mathbf{J} \boldsymbol{H} \end{pmatrix} \tag{1.2}$$

where $\mathbf{I}$ is the 2×2 identity matrix and where

$$\mathbf{G} = G\mathbf{I}, \quad \mathbf{K} = K\mathbf{J}, \quad \mathbf{F} = F\mathbf{I}, \quad \mathbf{L} = L\mathbf{J}$$

[3] $\boldsymbol{e}_x$,$\boldsymbol{e}_x$,$\boldsymbol{e}_z$ is the usual basis in $\mathbb{R}^3$.

2 Wave splitting

The wave splitting is a change of the dependent variables such that the new variables represent the general left- and right-going waves in a medium without dispersion, e.g., outside the slab. The idea of wave splitting has been used in several scattering problems, e.g., [1, 2, 11, 12]. Here, the same splitting as in an earlier paper, see [9], is used, i.e., the linear map

$$\begin{pmatrix} \boldsymbol{E}^+(z,t) \\ \boldsymbol{E}^-(z,t) \end{pmatrix} = \mathbf{P} \begin{pmatrix} \boldsymbol{E}(z,t) \\ \eta \mathbf{J} \boldsymbol{H}(z,t) \end{pmatrix} \tag{2.1}$$

where the 4×4 matrix $\mathbf{P}$ is defined as

$$\mathbf{P} = \frac{1}{2} \begin{pmatrix} \mathbf{I} & -\mathbf{I} \\ \mathbf{I} & \mathbf{I} \end{pmatrix}$$

is adopted. Note that $\boldsymbol{E}^{\pm}(z,t)$ are continuous at the boundaries of the slab, i.e., on the planes $z = 0$ and $z = d$, and hence they are continuous vector fields.

Outside the slab, $\boldsymbol{E}^{\pm}(z,t)$ are the electric fields of the general right- and left-going waves, respectively. Inside the slab, no interpretation in right- and left-going waves is possible, but the definition (2.1) is, nevertheless, well defined everywhere, and

$$\begin{cases} \boldsymbol{E}(z,t) = \boldsymbol{E}^+(z,t) + \boldsymbol{E}^-(z,t) \\ \boldsymbol{H}(z,t) = \dfrac{1}{\eta} \mathbf{J} \left(\boldsymbol{E}^+(z,t) - \boldsymbol{E}^-(z,t) \right) \end{cases}$$

3 Dynamics

The fields satisfy the system of equations in (1.2). The plus and minus fields $\boldsymbol{E}^+(z,t)$ and $\boldsymbol{E}^-(z,t)$, defined in Section 2, satisfy a similar system of equations. These equations are equivalent to (1.2) and straightforward to derive using (1.2) and (2.1). The result is

$$c \frac{\partial}{\partial z} \begin{pmatrix} \boldsymbol{E}^+ \\ \boldsymbol{E}^- \end{pmatrix} = \begin{pmatrix} -\mathbf{I} & \mathbf{0} \\ \mathbf{0} & \mathbf{I} \end{pmatrix} \frac{\partial}{\partial t} \begin{pmatrix} \boldsymbol{E}^+ \\ \boldsymbol{E}^- \end{pmatrix} + \begin{pmatrix} -\mathbf{G} - \mathbf{K} & -\mathbf{F} + \mathbf{L} \\ \mathbf{F} + \mathbf{L} & \mathbf{G} - \mathbf{K} \end{pmatrix} * \frac{\partial}{\partial t} \begin{pmatrix} \boldsymbol{E}^+ \\ \boldsymbol{E}^- \end{pmatrix}$$

The first term gives the dynamics for the free space contribution, and the second the perturbation due to the dispersion in the slab.

Propagation of singularities gives information about the rotation and the attenuation of the wave front as it propagates through the medium. Assume there is a finite jump discontinuity in the plus field $\boldsymbol{E}^+$ at $z = 0$. This finite jump discontinuity propagates through the medium and the finite jump discontinuity at depth z is related to its value at $z = 0$ as

$$\left[\boldsymbol{E}^+(z, t + z/c) \right] = \mathbf{Q}(0,z) \left[\boldsymbol{E}^+(0,t) \right]$$

where the 2×2 matrix $\mathbf{Q}(0,z)$ quantifies the rotation and the attenuation of the discontinuity. The square bracket $\left[\boldsymbol{E}^+(z, t + z/c) \right]$ denotes the finite jump discontinuity of the field at the point $(z, t + z/c)$, i.e.

$$\left[\boldsymbol{E}^+(z, t + z/c) \right] = \boldsymbol{E}^+(z, t + z/c + 0) - \boldsymbol{E}^+(z, t + z/c - 0)$$

The field $\boldsymbol{E}^-$ shows no finite jump discontinuity of this kind and therefore the total field $\boldsymbol{E}$ has exactly the same finite jump discontinuity as the field $\boldsymbol{E}^+$ above. Notice also, that the finite jump discontinuity $\left[\boldsymbol{E}^+(0,t)\right]$ is the same on either side of the interface of the slab.

The matrix $\mathbf{Q}(0,z)$ can be explicitly solved and expressed in the following general notation, see Ref. [9]:

$$\mathbf{Q}(z_1,z_2) = \exp\big(a(z_1,z_2)\big) \begin{pmatrix} \cos\phi(z_1,z_2) & -\sin\phi(z_1,z_2) \\ \sin\phi(z_1,z_2) & \cos\phi(z_1,z_2) \end{pmatrix} \tag{3.1}$$

where the angle of rotation of the wave front $\phi(z_1,z_2)$ is

$$\phi(z_1,z_2) = -\frac{1}{c}\int_{z_1}^{z_2} K(z',0)\,dz'$$

and the attenuation factor $a(z_1,z_2)$ is

$$a(z_1,z_2) = -\frac{1}{c}\int_{z_1}^{z_2} G(z',0)\,dz' \tag{3.2}$$

Notice that this result holds for an inhomogeneous slab with arbitrary susceptibility kernels $G(z,t)$, $F(z,t)$, $K(z,t)$ and $L(z,t)$.

4 The scattering operators

By use of linearity, causality and time-invariance, the scattering operators that relate the incident field $\boldsymbol{E}^+(0,t)$ to the reflected field $\boldsymbol{E}^-(0,t)$ and the transmitted field $\boldsymbol{E}^+(d,t+d/c)$ must be of the form

$$\begin{cases} \boldsymbol{E}^-(0,t) = \big(\mathbf{R}_{\mathrm{ph}}(\cdot) * \boldsymbol{E}^+(0,\cdot)\big)(t) \\ \boldsymbol{E}^+(d,t+d/c) = \mathbf{Q}(0,d)\left\{\boldsymbol{E}^+(0,t) + \big(\mathbf{T}_{\mathrm{ph}}(\cdot) * \boldsymbol{E}^+(0,\cdot)\big)(t)\right\} \end{cases} \tag{4.1}$$

where $\mathbf{R}_{\mathrm{ph}}(t)$ and $\mathbf{T}_{\mathrm{ph}}(t)$ are the physical reflection and transmission kernels, respectively, and $\mathbf{Q}(0,d)$ defined in (3.1).

By the axial symmetry of the problem, it is obvious that the form of the scattering operators is

$$\mathbf{R}_{\mathrm{ph}}(t) = \begin{pmatrix} R_1^{\mathrm{ph}}(t) & -R_2^{\mathrm{ph}}(t) \\ R_2^{\mathrm{ph}}(t) & R_1^{\mathrm{ph}}(t) \end{pmatrix}, \qquad \mathbf{T}_{\mathrm{ph}}(t) = \begin{pmatrix} T_1^{\mathrm{ph}}(t) & -T_2^{\mathrm{ph}}(t) \\ T_2^{\mathrm{ph}}(t) & T_1^{\mathrm{ph}}(t) \end{pmatrix} \tag{4.2}$$

It is easy to see that all 2×2 matrices of this form commute.

5 The Imbedding equations

The wave splitting naturally leads to the study of a subsection $[z,d]$ of the slab $[0,d]$. For each subsection the reflection and transmission imbedding kernels are defined by

$$\begin{cases} \boldsymbol{E}^-(z,t) = \big(\mathbf{R}(z,\cdot) * \boldsymbol{E}^+(z,\cdot)\big)(t) \\ \boldsymbol{E}^+(d,t+(d-z)/c) = \mathbf{Q}(z,d)\left\{\boldsymbol{E}^+(z,t) + \big(\mathbf{T}(z,\cdot) * \boldsymbol{E}^+(z,\cdot)\big)(t)\right\} \end{cases}$$

where

$$\mathbf{R}(z,t)=\begin{pmatrix}R_1(z,t) & -R_2(z,t)\\ R_2(z,t) & R_1(z,t)\end{pmatrix},\qquad \mathbf{T}(z,t)=\begin{pmatrix}T_1(z,t) & -T_2(z,t)\\ T_2(z,t) & T_1(z,t)\end{pmatrix}$$

due to axial symmetry. By continuity of the split vector fields, the following boundary values are obtained:

$$\begin{cases}\mathbf{R}(0,t)=\mathbf{R}_{\rm ph}(t)\\ \mathbf{T}(0,t)=\mathbf{T}_{\rm ph}(t)\end{cases},\qquad \begin{cases}\mathbf{R}(d,t)=\mathbf{0}\\ \mathbf{T}(d,t)=\mathbf{0}\end{cases}$$

The subsection problem generates a one parameter family of reflection and transmission kernels, which satisfy integro-differential equations. These imbedding equations are for the reflection kernel

$$\begin{aligned}&c\partial_z\mathbf{R}-2\partial_t\mathbf{R}=\partial_t\left\{\mathbf{F}+\mathbf{L}+2\mathbf{G}*\mathbf{R}+(\mathbf{F}-\mathbf{L})*\mathbf{R}*\mathbf{R}\right\}\\ &\mathbf{R}(d,t)=\mathbf{0}\\ &\mathbf{R}(z,+0)=-\big(\mathbf{F}(z,+0)+\mathbf{L}(z,+0)\big)/2\\ &[\mathbf{R}(z,2(d-z)/c)]=\frac{\exp\big(2a(z,d)\big)}{2}\big(\mathbf{F}(d,+0)+\mathbf{L}(d,+0)\big)\end{aligned}\tag{5.1}$$

and for the transmission kernel the result is

$$\begin{aligned}&c\partial_z\mathbf{T}=\partial_t\left\{\mathbf{G}+\mathbf{K}\right\}*\mathbf{T}+\partial_t\left\{\mathbf{G}+\mathbf{K}+(\mathbf{F}-\mathbf{L})*(\mathbf{R}+\mathbf{R}*\mathbf{T})\right\}\\ &\mathbf{T}(d,t)=\mathbf{0}\\ &2c\mathbf{T}(z,+0)=\int_z^d\left\{\mathbf{F}^2-\mathbf{L}^2-2\partial_t(\mathbf{G}+\mathbf{K})\right\}(z',+0)\,dz'\end{aligned}\tag{5.2}$$

The attenuation factor $a(z,d)$ is defined in (3.2). The domain of definition for these equations is $\{(z,t):t>0,\,0<z<d$ and $t\neq 2(d-z)/c\}$.

If the medium is reciprocal, i.e., $L(z,t)=0$, equation (5.1) shows that the cross-polarized reflection kernel $R_2(z,t)=0$. The reason for this is that the imbedding equation (5.1) then has only diagonal entries and no off-diagonal terms (this assumes unique solubility of the equation). The reflection kernel then simplifies to $\mathbf{R}(z,t)=R_1(z,t)\mathbf{I}$. As a consequence of this, the cross-polarized part of the reflected electric field from the finite or semi-infinite reciprocal bi-isotropic slab will be zero even if the slab is inhomogeneous. This result holds for any susceptibility kernels G, F and K and is therefore a general result. If also $F(z,t)=0$, then $\mathbf{R}=\mathbf{0}$, irrespective of the susceptibility kernel $G(z,t)$. This reflects the ill-posedness of the inverse scattering problem, since infinitely many dispersive profiles give the same reflection kernel $\mathbf{R}(z,t)$, i.e., the same reflected field regardless of the incident field. Transmission data can be used to resolve this non-uniqueness.

6 The Green Functions

In the previous section the scattering problem was analyzed using imbedding arguments. In this section an independent approach—the Green function equations—is

applied. The Green functions give the internal fields due to a delta function excitation. They are defined by

$$\begin{cases} \boldsymbol{E}^+(z,t+z/c) = \mathbf{Q}(0,z)\boldsymbol{E}^+(0,t) + \big(\mathbf{G}^+(z,\cdot) * \mathbf{Q}(0,z)\boldsymbol{E}^+(0,\cdot)\big)(t) \\ \boldsymbol{E}^-(z,t+z/c) = \big(\mathbf{G}^-(z,\cdot) * \mathbf{Q}(0,z)\boldsymbol{E}^+(0,\cdot)\big)(t) \end{cases}$$

where due to axial symmetry

$$\mathbf{G}^\pm(z,t) = \begin{pmatrix} G_1^\pm(z,t) & -G_2^\pm(z,t) \\ G_2^\pm(z,t) & G_1^\pm(z,t) \end{pmatrix}$$

By continuity of the split vector fields, the Green functions are related to the physical reflection and transmission kernels, i.e., the boundary conditions are

$$\begin{cases} \mathbf{G}^+(0,t) = \mathbf{0} \\ \mathbf{G}^-(0,t) = \mathbf{R}_{\mathrm{ph}}(t) \end{cases}, \qquad \begin{cases} \mathbf{G}^+(d,t) = \mathbf{T}_{\mathrm{ph}}(t) \\ \mathbf{G}^-(d,t) = \mathbf{0} \end{cases}$$

Analogous to the imbedding equations for the scattering kernels of the subsection problem, the Green functions satisfy a system of integro-differential equations. These equations, linear in $\mathbf{G}^\pm$, are for the matrix function $\mathbf{G}^+$

$$\begin{aligned} & c\partial_z\mathbf{G}^+ = -\partial_t\{\mathbf{G}+\mathbf{K}\} * \mathbf{G}^+ - \partial_t\big\{\mathbf{G}+\mathbf{K}+(\mathbf{F}-\mathbf{L})*\mathbf{G}^-\big\} \qquad (6.1) \\ & \mathbf{G}^+(0,t) = \mathbf{0} \\ & 2c\mathbf{G}^+(z,+0) = \int_0^z \big\{\mathbf{F}^2 - \mathbf{L}^2 - 2\partial_t(\mathbf{G}+\mathbf{K})\big\}(z',+0)\,dz' \end{aligned}$$

and for the matrix function $\mathbf{G}^-$

$$\begin{aligned} & c\partial_z\mathbf{G}^- - 2\partial_t\mathbf{G}^- = 2\mathbf{G}(z,0)\mathbf{G}^- + \partial_t\{\mathbf{F}+\mathbf{L}\} \\ & \qquad\qquad + \partial_t\big\{(\mathbf{F}+\mathbf{L})*\mathbf{G}^+\big\} + \partial_t\{\mathbf{G}-\mathbf{K}\}*\mathbf{G}^- \qquad (6.2) \\ & \mathbf{G}^-(d,t) = \mathbf{0} \\ & \mathbf{G}^-(z,+0) = -\big(\mathbf{F}(z,+0)+\mathbf{L}(z,+0)\big)/2 \\ & [\mathbf{G}^-(z,2(d-z)/c)] = \frac{\exp\big(2a(z,d)\big)}{2}\big(\mathbf{F}(d,+0)+\mathbf{L}(d,+0)\big) \end{aligned}$$

As in the imbedding formulation, the domain of definition in both these cases is $\{(z,t) : t > 0,\ 0 < z < d \text{ and } t \neq 2(d-z)/c\}$.

The explicit relation between the imbedding kernels $\mathbf{R}$ and $\mathbf{T}$ and Green functions is

$$\begin{cases} \mathbf{G}^+(d,t) = \mathbf{G}^+(z,t) + \mathbf{T}(z,t) + \big(\mathbf{T}(z,\cdot) * \mathbf{G}^+(z,\cdot)\big)(t) \\ \mathbf{G}^-(z,t) = \mathbf{R}(z,t) + \big(\mathbf{R}(z,\cdot) * \mathbf{G}^+(z,\cdot)\big)(t) \end{cases}$$

since all matrices commute.

7 The direct and inverse problems

In this section the direct and inverse scattering problems are addressed. All analysis in the preceding sections holds for a stratified slab, i.e., the susceptibility kernels vary with the depth z. In this section, however, the slab is assumed to be homogeneous. The inverse problem is therefore a reconstruction of functions depending only on the time t, i.e., to find the susceptibility kernels $G(t)$, $F(t)$, $K(t)$ and $L(t)$.

In the direct problem, the susceptibility functions $G(t)$, $K(t)$, $F(t)$ and $L(t)$ are known, and the scattering kernels $\mathbf{R}_{\text{ph}}(t)$ and $\mathbf{T}_{\text{ph}}(t)$ are sought. With these kernels the scattered fields can be calculated for any excitation, see (4.1). The internal fields can be calculated with the Green functions $\mathbf{G}^{\pm}(z,t)$. These direct problems have been addressed in two previous papers, see Refs. [8, 9]. Even though this paper emphasizes the inverse problem the solution of the direct scattering problem is used to reconstruct the dispersive profile.

In the inverse problem the kernels $\mathbf{R}_{\text{ph}}(t)$ and $\mathbf{T}_{\text{ph}}(t)$ and the matrix $\mathbf{Q}(0,d)$ are assumed to be known. These scattering kernels are obtained from the scattered fields by deconvolving (4.1). The unknowns in the inverse problem are four susceptibility kernels $G(t)$, $K(t)$, $F(t)$ and $L(t)$. Karlsson [4, 5] has shown that the forward algorithm can be used to solve the inverse problem for an isotropic dispersive medium. This method is a constructive method and does not use optimization. An outline of a generalization of this method is given below. To avoid bias in the solution of the inverse scattering problem, the imbedding equations are used to generate synthetic scattering data $\mathbf{R}_{\text{ph}}(t)$ and $\mathbf{T}_{\text{ph}}(t)$. The inverse scattering problem is then solved using the Green function formulations.

The method of Karlsson can be extended and used to solve the inverse scattering problem for a dispersive bi-isotropic medium. The outline of this extended Karlsson's method is:

Time step 0: Since $\mathbf{Q}(0,d)$ is assumed to be known through the transmission data, the initial values $G(0)$ and $K(0)$ are known, and the other initial values easily follow from

$$\begin{cases} \mathbf{F}(0) + \mathbf{L}(0) = -2\mathbf{R}_{\text{ph}}(0) \\ \mathbf{G}'(0) + \mathbf{K}'(0) = \dfrac{1}{2}(\mathbf{F}(0)^2 - \mathbf{L}(0)^2) - \dfrac{c}{d}\mathbf{T}_{\text{ph}}(0) \\ \mathbf{F}'(0) + \mathbf{L}'(0) = -2(\mathbf{R}'_{\text{ph}}(0) + \mathbf{G}(0)\mathbf{R}_{\text{ph}}(0)) \end{cases}$$

These initial values are easily found from the results above, see (5.1) and (5.2) or (6.1) and ().

Time step J: Suppose that $G'(j)$, $K'(j)$, $F'(j)$ and $L'(j)$[4] are known for time $j < J$. Analysis of the discretized version of the Green functions equations[5], (6.1) and (), for the direct scattering problem using the trapezoidal rule implies that

$$\begin{cases} \mathbf{T}_{\text{ph}}(J) = \mathbf{A}^{+}(J)\mathbf{G}'(J) + \mathbf{B}^{+}(J)\mathbf{K}'(J) + \mathbf{C}^{+}(J)\mathbf{F}'(J) + \mathbf{D}^{+}(J)\mathbf{L}'(J) + \mathbf{E}^{+}(J) \\ \mathbf{R}_{\text{ph}}(J) = \mathbf{A}^{-}\mathbf{G}'(J) + \mathbf{B}^{-}\mathbf{K}'(J) + \mathbf{C}^{-}\mathbf{F}'(J) + \mathbf{D}^{-}\mathbf{L}'(J) + \mathbf{E}^{-}(J) \end{cases}$$

[4] $G'(j) = \frac{d}{dt}G(j\Delta t)$ etc.

[5] The same conclusion can be made from (5.1) and (5.2) if the imbedding equations are used to solve the inverse scattering problem.

The coefficient matrices $\mathbf{A}^-$, $\mathbf{B}^-$, $\mathbf{C}^-$ and $\mathbf{D}^-$ are constant matrices and their explicit values are easily found. The matrices $\mathbf{A}^+$, $\mathbf{B}^+$, $\mathbf{C}^+$, $\mathbf{D}^+$, $\mathbf{E}^+$ and $\mathbf{E}^-$ depend only on $G'(j)$, $K'(j)$, $F'(j)$ and $L'(j)$ for time $j < J$, and vary, as indicated, with J. All matrices in this expression have the form as in (4.2) and therefore they all commute.

Thus, by running the forward program five times (four times in the reciprocal case) for different sets of $G'(J)$, $K'(J)$, $F'(J)$, $L'(J)$ at time J, a linear system of equations in the unknown coefficient matrices is obtained. After calculating these matrices, a linear system of equations in $G'(J)$, $K'(J)$, $F'(J)$ and $L'(J)$ is achieved. This system of equations can be solved since $\mathbf{T}_{\mathrm{ph}}(J)$ and $\mathbf{R}_{\mathrm{ph}}(J)$ are known. Finally, the Green functions $\mathbf{G}^{\pm}$ at all grid points for $j = J$ are computed by running the forward program once again. The procedure is then repeated for the next time step $J + 1$.

Two explicit examples in the next section illustrate the numerical performance of this algorithm.

8 Numerical results

In the following explicit examples, all frequencies (i.e., all numerical values) are given in units of c/d and time t in units of d/c.

Example 1

In this first example, a reciprocal multi-frequency Lorentz medium is presented. The susceptibility kernels are

$$\begin{cases} G(t) = 0.5e^{-0.2t}\sin 5t + 0.25e^{-0.5t}\sin 10t \\ F(t) = 0.5e^{-0.2t}\sin 5t + 0.2e^{-0.5t}\sin 10t \\ K(t) = 0.01e^{-0.5t}\cos 10t \\ L(t) = 0 \end{cases}$$

Since the medium is reciprocal ($L(t) = 0$), there is no cross coupling in the reflected field ($R_2^{\mathrm{ph}}(t) = 0$). The susceptibility kernels are shown in Figures 1 and 2. Notice that the chirality of the medium, modeled by $K(t)$, is two orders of magnitude smaller than the kernel $G(t) + F(t)$. This reduction of magnitude in the chirality kernel is believed to model realistic data. The reflection and transmission data for this medium are shown in Figure 3. The scattering data are continuous functions of t, since $F(0) = L(0) = 0$. The reconstructions of the susceptibility kernels are shown in Figures 1 and 2. In these reconstructions 64 data points per round trip ($t = 2$) are used.

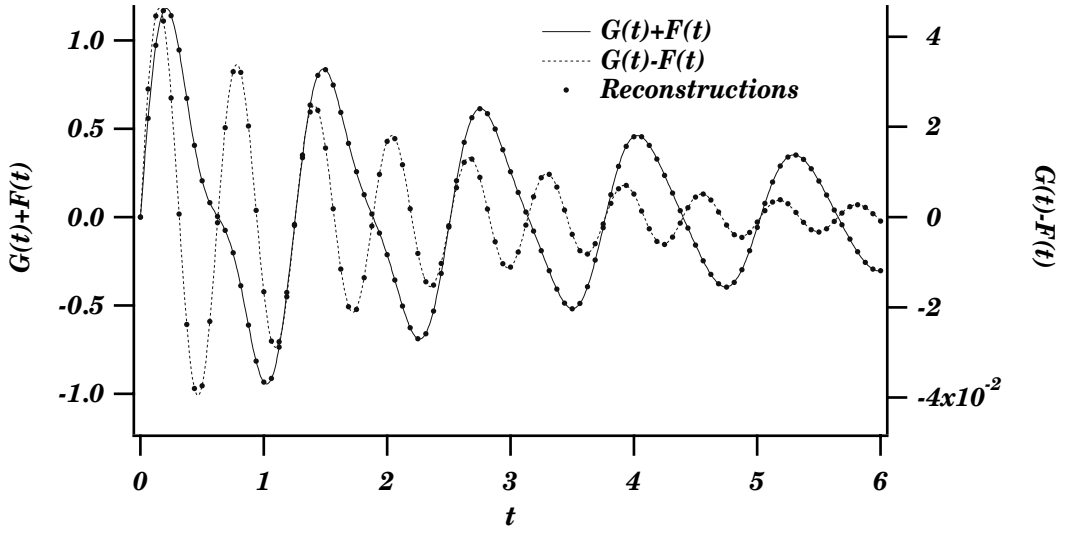

Figure 1: The susceptibility kernels $G(t) + F(t)$ and $G(t) - F(t)$ for the reciprocal Lorentz medium in Example 1 and their reconstructions. The time scale is given in units of d/c, and the vertical axis in units of c/d.

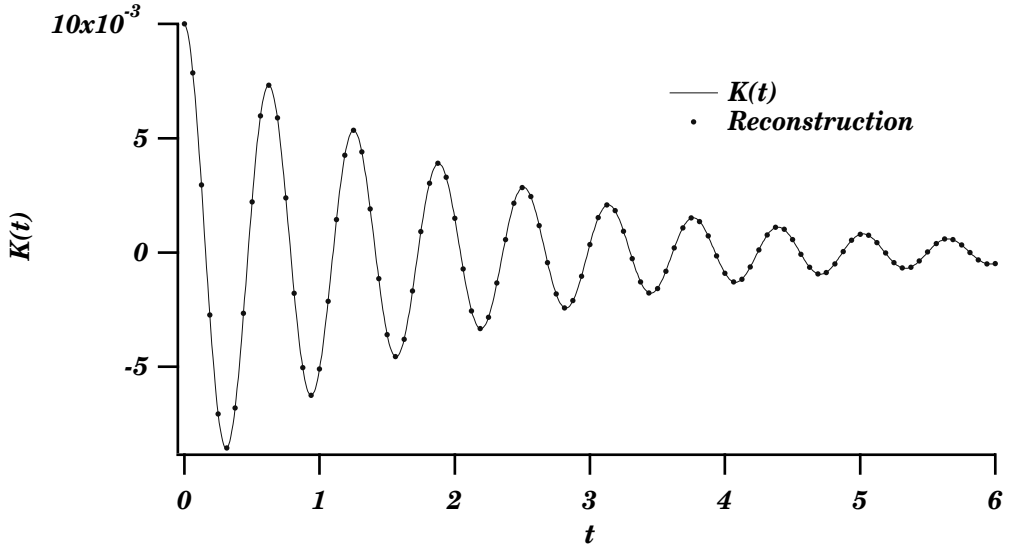

Figure 2: The susceptibility kernel $K(t)$ for the reciprocal Lorentz medium ($L(t) = 0$) in Example 1 and its reconstruction. The time scale is given in units of d/c, and the vertical axis in units of c/d.

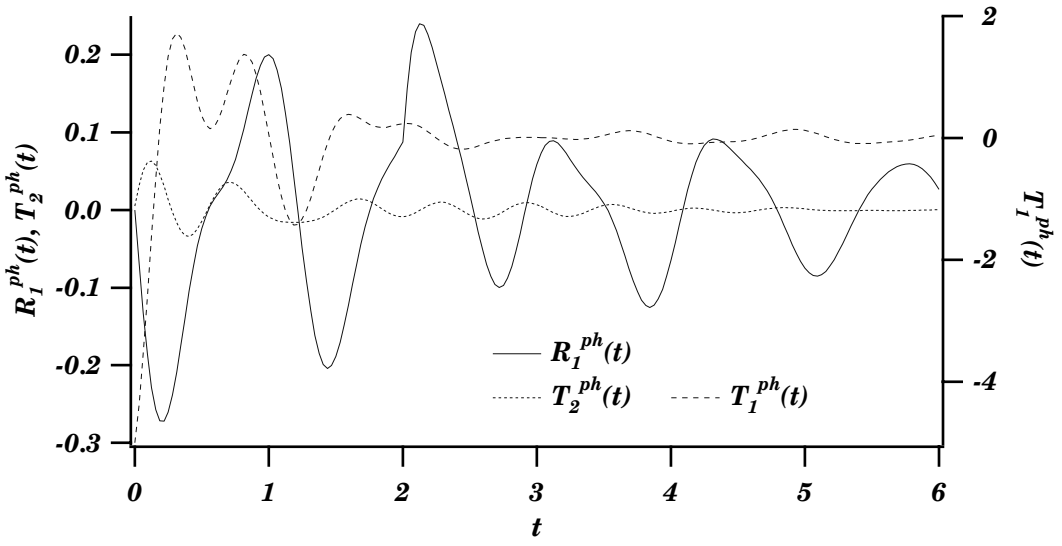

Figure 3: The reflection kernel $R_1^{\rm ph}(t)$ and the transmission kernels $T_1^{\rm ph}(t)$ and $T_2^{\rm ph}(t)$ for the reciprocal Lorentz medium ($R_2^{\rm ph}(t) = 0$) in Example 1. The time scale is given in units of d/c, and the vertical axis in units of c/d.

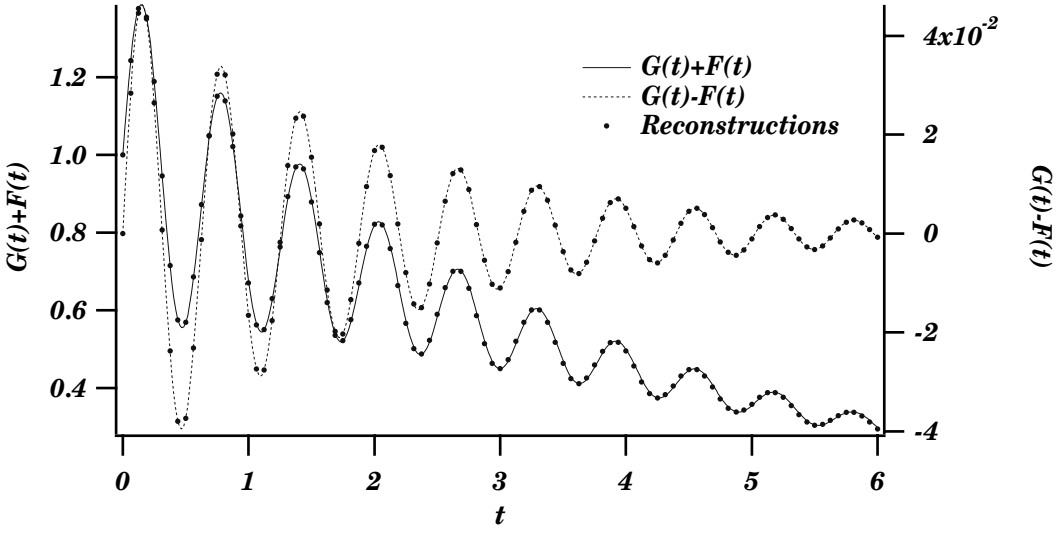

Figure 4: The susceptibility kernels $G(t) + F(t)$ and $G(t) - F(t)$ for the Debye-Lorentz medium in Example 2 and their reconstructions. The time scale is given in units of d/c, and the vertical axis in units of c/d.

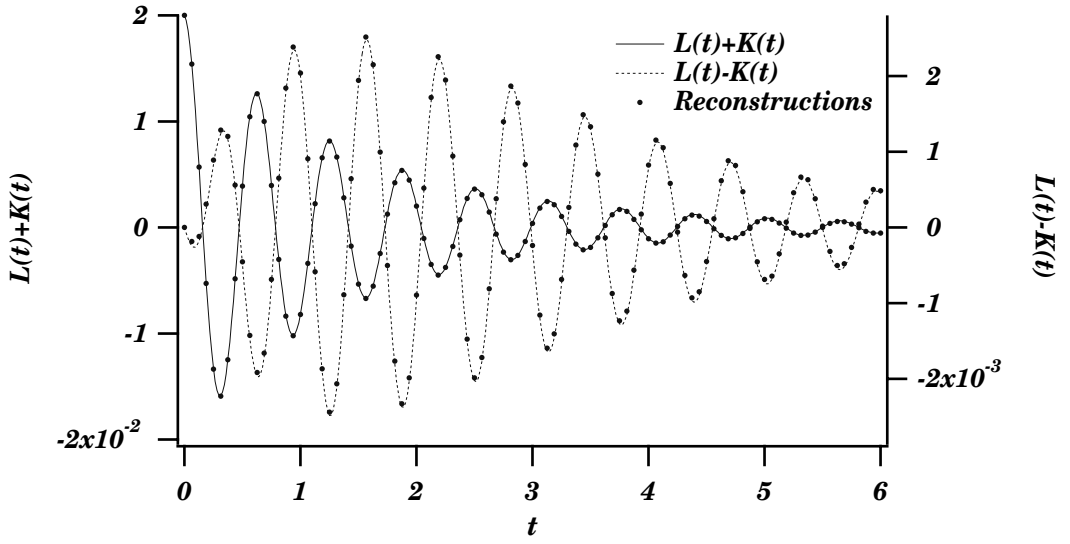

Figure 5: The susceptibility kernels $L(t) + K(t)$ and $L(t) - K(t)$ for the Debye-Lorentz medium in Example 2 and their reconstructions. The time scale is given in units of d/c, and the vertical axis in units of c/d.

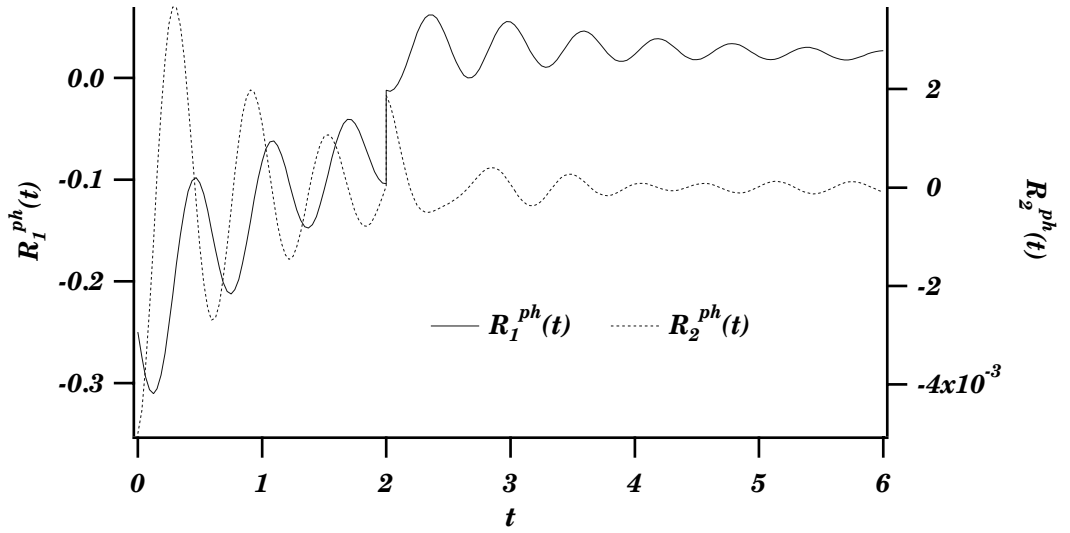

Figure 6: The reflection kernels $R_1^{\rm ph}(t)$ and $R_2^{\rm ph}(t)$ for the Debye-Lorentz medium in Example 2. The time scale is given in units of d/c, and the vertical axis in units of c/d. Notice the finite jump discontinuity in $R_1^{\rm ph}(t)$ and $R_2^{\rm ph}(t)$ at one round trip $t = 2$.

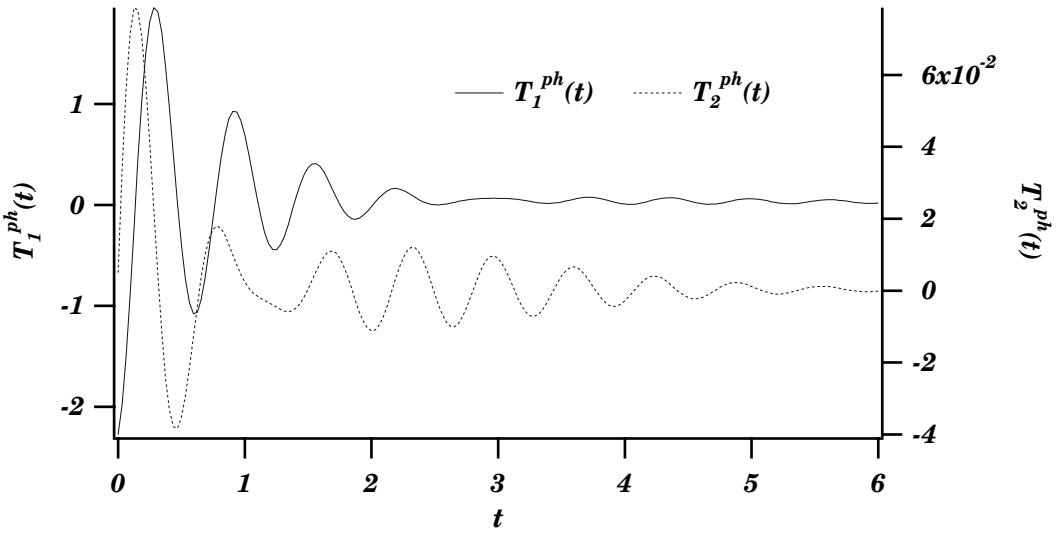

Figure 7: The transmission kernels $T_1^{\mathrm{ph}}(t)$ and $T_2^{\mathrm{ph}}(t)$ for the Debye-Lorentz medium in Example 2. The time scale is given in units of d/c, and the vertical axis in units of c/d.

Example 2

The second example is a non-reciprocal multi-frequency Debye-Lorentz medium. These susceptibility kernels are

$$\begin{cases} G(t) = 0.5e^{-0.2t} + 0.25e^{-0.5t}\sin 10t \\ F(t) = 0.5e^{-0.2t} + 0.2e^{-0.5t}\sin 10t \\ K(t) = 0.01e^{-0.5t}\cos 10t \\ L(t) = 0.01e^{-t}\cos 10t \end{cases}$$

The susceptibility kernels are depicted in Figures 4 and 5. The reflection and transmission data for this medium are shown in Figures 6 and 7. As in Example 1, the chirality of the medium is two orders of magnitude smaller than the kernel $G(t) + F(t)$. Notice that the reflection kernels $R_1^{\mathrm{ph}}(t)$ and $R_2^{\mathrm{ph}}(t)$ have finite jump discontinuities at one round trip ($t = 2$), since $F(0), L(0) \neq 0$. The reconstructions of the susceptibility kernels are shown in Figures 4 and 5. In these reconstructions 64 data points per round trip ($t = 2$) are used.

Both these numerical experiments show that excellent reconstructions of the susceptibility kernels $G(t)$, $F(t)$, $K(t)$ and $L(t)$ are obtained.

References

[1] J.P. Corones, M.E. Davison, and R.J. Krueger. Direct and inverse scattering in the time domain via invariant imbedding equations. *J. Acoust. Soc. Am.*, **74**(5), 1535–1541, 1983.

[2] J.P. Corones, M.E. Davison, and R.J. Krueger. Wave splittings, invariant imbedding and inverse scattering. In A.J. Devaney, editor, *Inverse Optics*, pages 102–106, SPIE Bellingham, WA, 1983. Proc. SPIE 413.

[3] N. Engheta and D.L. Jaggard. Electromagnetic chirality and its applications. *IEEE Antennas and Propagation Society Newsletter*, pages 6–12, October 1988.

[4] A. Karlsson. Inverse scattering for viscoelastic media using transmission data. *Inverse Problems*, **3**, 691–709, 1987.

[5] A. Karlsson. Direct and inverse electromagnetic scattering from a dispersive medium. Technical Report TRITA-TET 89-2, Department of Electromagnetic Theory, S-100 44 Stockholm, Sweden, 1989.

[6] A. Karlsson and G. Kristensson. Constitutive relations, dissipation and reciprocity for the Maxwell equations in the time domain. *J. Electro. Waves Applic.*, **6**(5/6), 537–551, 1992.

[7] G. Kristensson and R.J. Krueger. Direct and inverse scattering in the time domain for a dissipative wave equation. part 3: Scattering operators in the presence of a phase velocity mismatch. *J. Math. Phys.*, **28**(2), 360–370, 1987.

[8] G. Kristensson and S. Rikte. Scattering of transient electromagnetic waves in reciprocal bi-isotropic media. Technical Report LUTEDX/(TEAT-7015)/1–17/(1991), Lund Institute of Technology, Department of Electromagnetic Theory, P.O. Box 118, S-211 00 Lund, Sweden, 1991. *J. Electro. Waves Applic.* (in press).

[9] G. Kristensson and S. Rikte. Transient wave propagation in reciprocal bi-isotropic media at oblique incidence. Technical Report LUTEDX/(TEAT-7019)/1–25/(1992), Lund Institute of Technology, Department of Electromagnetic Theory, P.O. Box 118, S-211 00 Lund, Sweden, 1992. *J. Math. Phys.* (accepted for publication).

[10] A. Lakhtakia. Recent contributions to classical electromagnetic theory of chiral media: what next? *Speculations in Science and Technology*, **14**(1), 2–17, 1991.

[11] V.H. Weston. Invariant imbedding for the wave equation in three dimensions and the applications to the direct and inverse problems. *Inverse Problems*, **6**, 1075–1105, 1990.

[12] V.H. Weston. Time-domain wave-splitting of Maxwell's equations. Technical Report LUTEDX/(TEAT-7016)/1–25/(1991), Lund Institute of Technology, Department of Electromagnetic Theory, P.O. Box 118, S-211 00 Lund, Sweden, 1991.